SLAC–PUB–5171
January 1990
(A)

# COMPUTER DETERMINATION OF THE EXTERNAL $Q$ AND RESONANT FREQUENCY OF WAVEGUIDE LOADED CAVITIES

**Norman M. Kroll**[⋆]
*University of California, San Diego*
*La Jolla, CA 92093*
*and*
*Stanford Linear Accelerator Center,*
*Stanford University, Stanford, CA 94309*

**David U. L. Yu**[⋆⋆]
*DULY Consultants*
*Rancho Palos Verdes, CA 90732*

**Abstract**

A new method is proposed for determining the $Q_{ext}$ of a cavity coupled to a wave guide that is well suited to integration with computer methods for determination of cavity resonant frequencies. It is related to, but distinct from, Slater's method, which recently has been applied in the same context. Application of the method to a set of waveguide models with comparison to analytic results is presented. An application to a damped accelerator cavity structure using MAFIA determined resonant frequencies is also given.

Submitted to *Particle Accelerators.*

⋆ Work supported by Department of Energy contracts DE–AC03–76SF00515, DE–AS03–89ER40527, and DE–AS03–81ER40029.
⋆⋆ Work supported by Department of Energy SBIR contract DE–AC03–87ER80529.

A number of powerful computer programs have been developed which are capable of computing the resonant frequencies of closed lossless cavity resonators. In addition, field distributions, cavity impedance, and $Q$ due to weak losses in walls and dielectrics are readily computed. Examples are MAFIA[1], URMEL[2], and SUPERFISH[3]. These programs have proved to be valuable tools for the design of cavities for accelerating structures and radio frequency power sources. These programs do not, however, have built in procedures for calculating the $Q$ due to coupling to an external waveguide. There is currently a strong interest in cavities which are heavily damped by external coupling. It is the purpose of this paper to develop procedures for calculating $Q_{ext}$ and resonant frequency which are reliable even when the external coupling is very strong.

It is clear from the work of Slater[4] that the desired information can be obtained by inserting a terminating short on the end of the waveguide and studying the behavior of the combined cavity, output structure, and waveguide as the distance of the terminating short from the end of the waveguide is varied. Gluckstern and Li[5] have described a computer method of applying the Slater method. Goren and Yu[6] have described an equivalent circuit approach and a simple computer method. We describe an alternate method here similar in character to the Slater method, but in our opinion simpler to derive and better suited to computer application.

## 1. BASIC THEORY

We consider a cavity coupled to a single waveguide of uniform cross-section. The generalization to many outputs is straightforward. Although the connection between the cavity and waveguide may be fairly complex as, for example, in the accelerating structure recently proposed by Palmer[7], we shall consider the cavity to end and the output to begin at the point where the cross-section of the output

waveguide becomes uniform. We refer to this point as the output origin[8]. Paralleling Slater we consider the waveguide to be shorted with a conducting plane at a distance from the output origin. One may think of the system as a cavity resonator and waveguide resonator coupled together through the output circuit. Typical examples of the dependance of the resonant frequencies of relevant modes on the shorting distance are shown in Figs. 1a and 1b. Fig. 1a exhibits the behavior when the external coupling is quite small ($Q_{ext} \approx 1600$). The dashed lines correspond to the wave guide modes present with no coupling between the waveguide and the cavity. The frequencies are all normalized to the frequency of the uncoupled cavity, so that the uncoupled cavity resonance is fixed at ordinate one. The solid curves, which represent the frequency of the coupled system when a small iris is opened between the cavity and waveguide, exhibit avoided crossing behavior near each point where the uncoupled waveguide and cavity mode curves would cross. Fig 1b exhibits the evolution of this behavior when the coupling is increased ($Q_{ext} \approx 38$). Our formulation will deal with frequency, $\omega$, as a function of $\psi$, the phase change along the guide, given by $2\pi D/\lambda_g$ where $\lambda_g$ is the guide wavelength and $D$ is the waveguide length. This behavior (for the Fig. 1b case) is illustrated in Fig. 2. The $\psi - \omega$ curves corresponding to the various curves of Fig. 1a or 1b differ from one another only by additive multiples of $\pi$. Thus only one such curve is shown in Fig. 2. Fig. 3 (again for the Fig. 1b case) shows $G \equiv -(1/2)(d\psi/d\omega)$ plotted as a function of $\omega$. All of the $\psi - \omega$ curves produce a single $G$ curve. The $G$ curve exhibits a typical resonance form, and we shall see that the peak of this curve occurs at the resonant frequency of the cavity with the waveguide feeding into a matched load. When multiplied by the resonant frequency, the height of the curve, apart from a small correction to be discussed later, is equal to $Q_{ext}$. Since we shall be considering lossless cavities exclusively, there is no distinction between $Q_{ext}$ and $Q$, and we shall henceforth simply use $Q$.

In order to specify what we mean by the resonant frequency and $Q$ of our cavity, we consider the boundary value problem presented by the cavity with its waveguide output, which we now consider to be infinitely long. We assume perfect conductor boundary conditions on all of the walls. As one proceeds along the waveguide towards infinity the fields are required to approach those of the principal mode (assumed here to be the only one which can propagate without attenuation) propagating towards infinity (referred to henceforth as the outgoing wave boundary condition). The eigenmodes of such a system are complex, with positive imaginary part, corresponding to oscillations which are exponentially damped in time. Writing this eigenvalue as $u+jv$, we identify $u$ with the resonant frequency of the waveguide loaded cavity and $u/2v$ with the cavity $Q$. Many other definitions of these quantities have appeared in the literature, based on the properties of such things as resonance curves, and stored and dissipated (or radiated) energy concepts. Many of these require additional specifications in order to totally avoid ambiguity. While these issues can usually be ignored for typical situations, they may become signifigant in the case of very low $Q$'s. Our definition avoids such problems. Furthermore damping rate, which is equal to $v$ for field amplitudes, is usually an item of central interest for heavily loaded cavities. We also avoid the need for the specification of a reference plane as the concept does not appear in our specification of the boundary value problem[9].

While it would be most reliable and straightforward simply to computationally solve the eigenvalue problem defined above, programs having that capability have not to our knowledge been developed. We shall therefore proceed along the line suggested above and relate the $\psi - \omega$ curve of Fig. 2 to the resonance parameters $u$ and $v$.

The $z$ dependence of the transverse electric field between the waveguide origin and the shorting plane is of the form

$$e^{jkz} + Re^{-jkz}$$

where $k = 2\pi/\lambda_g$, $Z$ is distance along the waveguide axis, and $R$ is the reflection coefficient referred to the waveguide origin plane. Since it must vanish at $z = D$, the shorting plate position, it must also be proportional to

$$2jsin(kz - \psi - n\pi) = (e^{jkz} - e^{2j\psi}e^{-jkz})e^{-j\psi}$$

Comparing the two forms we see that $R = -exp(2j\psi)$. We now observe that because the eigen frequency corresponds to a situation in which there is an outgoing wave but no incoming wave, the reflection coefficient must have a pole there. This, combined with the fact that $R$ must have absolute value one for real values of $\omega$, means that it may be written

$$R(\omega) = -\frac{\omega - u + jv}{\omega - u - jv}e^{-2j\chi(\omega)} = -e^{2j\psi} \tag{1.1}$$

where $\chi(\omega)$ is a real function, analytic at $\omega = u + jv$. It represents non resonant effects, effects of distant resonances, and effects associated with the mode structure of the wave guide. We next take the logarithm of both sides of Eq. (1.1) to obtain

$$\psi(\omega) = tan^{-1}(\frac{v}{\omega - u}) - \chi(\omega) + n\pi \tag{1.2}$$

We shall assume that $\chi(\omega)$ can be adequately represented for real values of its argument in the vicinity of the resonance by the first two terms of its power series expansion about u. Thus we write

$$\chi(\omega) \cong \chi(u) + \chi'(u)(\omega - u) \tag{1.3}$$

Equation (1.3) is the basic approximation upon which our method is based. While, $\chi(\omega)$ can be approximately removed by application of the detuned short procedure[4],

we find it to be more convenient for computer application to determine it by fitting to the computed $\psi - \omega$ relation[10].

Differentiating Eq. (1.2) and applying Eq. (1.3) we find

$$-\frac{1}{2}\frac{d\psi}{d\omega} = \frac{1}{2}\frac{v}{(\omega-u)^2+v^2} + \frac{1}{2}\chi'(u). \tag{1.4}$$

It is apparent that Eq. (1.4) exhibits a typical resonant form with peak at $\omega = u$, and when multiplied by $u$, with peak value $Q + \frac{1}{2}u\chi'(u)$. The second term represents the correction that we mentioned earlier. It tends to be of order one while $Q$ is moderately large to quite large compared to one.

We note that Eq. (1.2) is unchanged when a reference plane other than the origin is selected. It is clear from the definition of the reflection coefficient that a shift in the reference plane a distance $d$ towards the incoming wave multiplies the expression for $R$ by a factor $exp(-2jkd)$, which is equivalent to changing $\chi(\omega)$ to $\chi(\omega) + kd$. On the other hand, the definition of $\psi$ changes from $kD$ to $k(D-d)$ so that the relation expressed by Eq. (1.2) is unaffected. The choice of reference plane can make a difference, however, when the approximation (1.3) is made. Because the dependence of k on frequency is not linear in a waveguide, a large value of $z$ could introduce a large error in (1.3). While we have no real reason to claim that $z = 0$ is the best choice, our experience to be discussed later shows that it is a satisfactory choice. The detuned short method attempts to choose the position of the reference plane in such a way (frequency dependent) that $\chi(\omega)$ is eliminated all together. As mentioned previously, we consider the implementation of the detuned short method to be less convenient computationally than the procedure which we are proposing[10].

The choice of representation of $R(\omega)$ by Eq. (1.1) is not unique. There may be situations in which it is useful, for instance, to exhibit two resonances. The resonances may be too close to the frequency of interest to make the approximate

Eq. 1.3 adequate in itself. Taking account of the fact that $R(\omega)$ has a pole in the complex plane at both resonances we replace Eq. (1.1) with

$$R(\omega) = -\frac{\omega - u_1 + jv_1}{\omega - u_1 - jv_1} \frac{\omega - u_2 + jv_2}{\omega - u_2 - jv_2} e^{-2j\chi(\omega)} = -e^{2j\psi} \tag{1.5}$$

Correspondingly Eq. (1.2) becomes

$$\psi(\omega) = tan^{-1}(\frac{v_1}{\omega - u_1}) + tan^{-1}(\frac{v_2}{\omega - u_2}) - \chi(\omega) + n\pi \tag{1.6}$$

$X(\omega)$ is now analytic at both poles and a linear approximation analogous to Eq. (1.3) would normally be employed.

## 2. IMPLEMENTATION FORMULAS

The expression (1.2) together with the approximation (1.3) provides a four parameter representation of the exact relation between $\psi$ and $\omega$. We shall refer to this representation as the four parameter formula. A set of computations with different values of $D$ provides a number of $\psi$-$\omega$ pairs. It is convenient to think of these pairs as data and to think of the determination of $u$ and $Q$ as arising from a four parameter fit to the data. Model calculations carried out in the next section will provide strong evidence that the four parameter formula provides an excellent representation of the exact relation. It will further be seen that for $Q$ values in excess of 20 a three parameter representation obtained by setting $\chi'(u)$ equal to zero is also excellent. Thus explicit formulas which determine $u$ and $Q$ from just three or four points are of interest.

We shall now show that for arbitrary choice of $\chi'(u)$, it is possible to obtain explicit expressions for $u, v$, and $\chi(u)$ such that the four parameter formula passes through any three points in the $\psi$-$\omega$ plane. Let us designate the three points by $(\psi_i, \omega_i)$ where $i = 1$, 2, or 3. Then from Eq. (1.2) and (1.3) we have

$$\psi_i + \chi(u) + \chi'(u)(\omega_i - u) = \tan^{-1}(\frac{v}{\omega_i - u}). \tag{2.1}$$

Taking the difference of the above for $i$=1 and $i$=2 yields

$$\psi_1 - \psi_2 + \chi'(u)(\omega_1 - \omega_2) = \tan^{-1}(\frac{v}{\omega_1 - u}) - tan^{-1}(\frac{v}{\omega_2 - u}). \tag{2.2}$$

Next take the tangent of both sides, use a standard trigonometric identity, and rearrange slightly to get

$$tan[\psi_1 - \psi_2 + \chi'(u)(\omega_1 - \omega_2)] = \frac{v(\omega_2 - \omega_1)}{(\omega_1 - u)(\omega_2 - u) + v^2.} \tag{2.3}$$

Now take the reciprocal and multiply by $(\omega_1 - \omega_2)$ to obtain

$$-(\omega_1 - \omega_2)cot[\psi_1 - \psi_2 + \chi'(u)(\omega_1 - \omega_2)] = -v - \frac{(\omega_1 - u)(\omega_2 - u)}{v} \equiv B_{12}. \tag{2.4}$$

Here we identify $B_{12}$ with the left hand side of (2.4) and note that it is completely determined by a pair of the originally designated points and the assumed value of $\chi'(u)$. Defining $B_{23}$ analogously we define

$$A \equiv \frac{B_{12} - B_{23}}{\omega_3 - \omega_1} \tag{2.5}$$

a quantity determined by the three designated points and $\chi'(u)$, and find, following simple algebra, that

$$\frac{(\omega_2 - u)}{v} = A. \tag{2.6}$$

Eq. (2.6) can be combined with (2.4) to eliminate $v$ and obtain

$$u = \frac{\omega_2 + AB_{12} + \omega_1 A^2}{1 + A^2}. \tag{2.7}$$

Now that $u$ has been determined, $v$ and $\chi(u)$ can be determined successively using, from (2.4) and (2.6)

$$v = (u - \omega_1)A - B_{12}, \tag{2.8}$$

and from (2.1)

$$\chi(u) = tan^{-1}\frac{v}{\omega_i - u} - \psi_i - \chi'(u)(\omega_i - u). \tag{2.9}$$

Any of the three points can be used in (2.9). Indeed, despite the unsymmetric appearance of the formulas, the results obtained for the parameters are independent of the designation of the points as 1,2,3. Eqs. (2.7), (2.8), and (2.9) show that the three parameters are (apart from the trivial $n\pi$ ambiguity in $\chi(u)$) uniquely determined by the three points and $\chi'(u)$. Thus if three points are computed from three values of $D$ and $\chi'(u)$is set equal to zero, one gets a three parameter fit of the resonance curve which passes through the three points and provides a value for $u$ and $Q$.

If a fourth point is provided by a fourth value of $D$, one can normally choose $\chi'(u)$ so that the parameterised representation passes through all four points. While neither a solution nor uniqueness is any longer guaranteed, in practice a solution will always be found. If there is more than one solution, it may be necessary to compute additional data points to determine which of the solutions best fits the additional points. Furthermore solutions which give negative values for $u$ or $v$ must be rejected.

In order to determine $\chi'(u)$, we use Eq. (2.1) with $i$=4, rearranged as follows.

$$\omega_4 - u - vcot[(\psi_4 + \chi(u) + \chi'(u)(\omega_4 - u)] = 0 \tag{2.10}$$

Since $u, v$, and $\chi(u)$ have all been determined by assuming a value for $\chi'(u)$, the left hand side of Eq. (2.10) can be regarded as a function of $\chi'(u)$, and $\chi'(u)$ is determined as a root of (2.10). The root or roots may be located approximately by computing (2.10) over a suitable range of values, and a simple numerical root finding procedure can be used to locate an accurate value of $\chi'(u)$.

In order to increase confidence in the results, one may wish to compute data points for additional values of $D$. One may then investigate the stability of the parameters with respect to the particular set of points chosen. Alternatively one may do a least squares fit to all of the computed points. We have carried out such fits based upon the left hand side of Eq. (2.10). The expression (with 4 replaced by $i$) is squared and summed over all the points. The resultant expression is then minimized with respect to the parameters. A numerical search procedure is required. The least squares fit method works even when the number of points equals the number of parameters, and thus could be used instead of the more straightforward method described above.

## 3. APPLICATION TO AN ANALYTICAL WAVEGUIDE MODEL

In order to assess the reliability of the approach described in 1 and 2, we have studied a resonator formed by placing a zero thickness conducting iris across a shorted waveguide. The wave guide is taken to be of standard rectangular form propagating in the standard $TE_{10}$ mode. The iris opening is centered with respect to the waveguide width with edges parallel to the electric field, a configuration referred to as a symmetric an inductive iris. The entire structure is illustrated in Fig. 4. Both the cavity and its output structure are intended to be electromagnetically similar to a Klystron cavity. With this in mind, we have chosen the cavity length and width to be equal. The coupling of the cavity to the wave guide output can be varied by varying the width of the opening in the iris window. Below the cutoff of the higher waveguide modes, the configuration shown in Fig. 4 can be rigorously

represented by the equivalent circuit shown in Fig. 5. The open waveguide with the outgoing wave boundary condition is represented in Fig. 5a, and the waveguide with variable short at distance $D$ from the iris is shown in Fig. 5b. The parallel lines represent transmission lines with propagation constant $k$ satisfying

$$k^2 = (\frac{\omega}{c})^2 - (\pi/a)^2.$$

While exact formulas for the shunt susceptance $B$ are not known, highly accurate expressions may be found in the Waveguide Handbook by Marcuvitz[11]. For our purposes, however, it will be sufficient to use the simpler, but less accurate expression[12] (normalized to the characteristic admittance of the waveguide)

$$B = -(\frac{2\pi}{ka})cot^2(\frac{\pi d}{2a}). \tag{3.1}$$

The object of our model is to compare the results of our implementation procedure applied to the Fig. 5b configuration with the coupled resonance parameters associated with the loaded cavity configuration in Fig. 5a. In addition we are interested in comparing our parameterised $\psi - \omega$ relation with the relation obtained from the equivalent circuit of Fig.5b. These objectives can be accomplished if the "data" used in the implementation formulas are obtained from the equivalent circuit using Eq. (3.1) and if (3.1) is used in both Fig. 5a and 5b. The other important point is that the analytic properties of our relations with the approximate (3.1) are quite similar to those with the more accurate expression that could be used and hence quite realistic. The equivalent circuits of Fig. 5 imply

$$cotka + \frac{2\pi}{ka}cot^2\frac{\pi d}{2a} + j = 0 \tag{3.2}$$

for the externally loaded cavity, and

$$cotka + \frac{2\pi}{ka} cot^2 \frac{\pi d}{2a} + cot(kD) = 0 \tag{3.3}$$

for the cavity with output shorted at distance $D$. To simplify our expressions and avoid reference to arbitrary dimensions, we work with frequency and wave number normalized to values associated with the closed waveguide cavity, $u_0$ and $k_0$ respectively. Thus we define $x = ka/\pi$ and note that

$$x^2 = 2(\frac{\omega}{u_0})^2 - 1.$$

With this change in notation we have the following three working relations

$$cot\pi x + \frac{2}{x} cot^2 \frac{\pi d}{2a} + j = 0, \tag{3.2'}$$

$$cot\pi x + \frac{2}{x} cot^2 \frac{\pi d}{2a} + cot(\pi x \frac{D}{a}) = 0, \tag{3.3'}$$

and

$$cot\pi x + \frac{2}{x} cot^2 \frac{\pi d}{2a} + cot\psi = 0, \tag{3.4}$$

with

$$x = [2(\omega/u_o)^2 - 1]^{\frac{1}{2}}. \tag{3.5}$$

Eq. (3.2') is to be regarded as a function of $\omega/u_o$. Its complex roots in this variable can be determined by a simple numerical procedure to as high an accuracy as desired. Hence it is used to determine the exact values of $u/u_o$, $v/u_o$, and hence $Q$. A simple one dimensional root finding procedure applied to (3.3') can be used to determine the $(u/u_o) - D$ relation for various modes. Fig. 1 was in fact obtained in this way. Eq (3.4) can be explicitly solved for $\psi$ in terms of $\omega/u_o$ and used to provide $\psi - (\omega/u_o)$ pairs for use in the formulas of § 2. Figs. 2 and 3 were obtained from Eq. (3.4) and its derivative with respect to $\omega/u_o$.

The results obtained in the comparison between the exact values of the resonance parameters and those obtained from the three and four parameter formulas are shown in Table I. By and large the frequencies used for determining the $\psi - \omega$ data points were first guesses and are listed in the last column of the table. While the four parameter formula gives more accurate results in every case, the agreement with the exact results is seen to be generally excellent for both. We have investigated the stability of the results with respect to the choice of frequencies and found that to be excellent as well. For example, in the case $d/a = 0.5$ selection of frequencies from the range 0.91 to 0.97 led to no variation whatever (to the accuracy of Table I) in $u$ or $Q$ for the 4 parameter formula. In the case of the three parameter formula $Q$ values varied over the range 22.9 to 24.9. Included in the comparison were cases in which the points used were all on one side of the resonance. Another example is provided by the $d/a = 0.65$ case. Here with points selected in the frequency range 0.83 to 0.97 the $Q$ variation was 7.94 to 8.00 in the 4 parameter case and 7.76 to 9.37 in the 3 parameter case. All cases were examined in a comparable way, and from the results obtained we conclude that the excellent agreement shown in Table I was not due to an accidentally propitious choice of frequencies for the determination of the data points.

Encouraged by the excellent results noted above, we have investigated the possibility of determining the resonance parameters by using only two waveguide lengths. Four useful data points can be obtained by choosing a pair of $D$ values near a region of avoided crossing and using the frequency values associated with each of the two branches exhibiting the avoided crossing behavior. For example, referring to Fig. 1b, the lower pair of curves at normalized length $R = 1.0$ and 1.1 might be used. The avoided crossing near $R = 2.0$ could be used instead. Because the data points are constrained to be further from the resonance pole in the complex plane than was typical of the examples of Table I, somewhat less accuracy would

be expected. However the stability of the results reported above suggests that the loss of accuracy may be quite small. This procedure has potential advantages for computer applications to real models, because a number of computer programs (e.g. URMEL and MAFIA) would yield both modes in the same run. Thus one could in principle determine the resonance parameters from only two runs provided that the lengths were chosen wisely. There is also a possibility that computer accuracy problems may be reduced with this procedure. The results of applying the method to the waveguide model are shown in Table II. We refer to the various curves of Fig. 1 as branches and number them 1,2,... in order of increasing frequency. It appears from Table II that the lowest two branches are satisfactory for the higher $Q$ cases, but that it is better to use branch 2 and 3 for the lower $Q$ cases. Overall, the quality of the results is quite comparable to those shown in Table I.

In order to investigate the accuracy with which the $\psi - \omega$ relation given by Eqs. (3.4) and (3.5) is modeled by its four parameter representation, we have computed the difference between $\psi$ as determined by Eqs. (1.2) and (1.3) using the parameters associated with the fits exhibited in Table I and the $\psi$ determined by Eqs. (3.4) and (3.5) as $\omega/u_o$ is varied from .71 to 1.15. The lower limit of the frequency range was determined by the proximity of the waveguide cutoff. The choice of upper limit was arbitrary. The fit was of course best in the vicinity of resonance and was of order $10^{-5}$ rad or better. Table III lists the range in line widths over which the deviation was less than 0.01 rad (and 0.1 rad for the very low $Q$ cases). The overall quality of the fit is consistent with the insensitivity of the parameters to the choice of fit points.

## 4. APPLICATION TO A DAMPED ACCELERATOR CAVITY MODEL

As discussed in the introduction, the method described in this paper was developed for use in conjunction with computer codes designed to determine the resonant frequencies of closed cavities. As a first example of its use in this manner we selected

a cavity designed by Robert Palmer[13] as a study model for an accelerator cavity with heavily damped transverse modes. The cavity had been built and studied experimentally. But with the experimental methods employed it was not possible to measure the $Q$ unambiguously. Although there was confusion due to overlap of the very broad resonance with a narrow resonance, it was concluded that the $Q$ of the principal deflecting mode was probably between 10 and 20.

A schematic drawing of the configuration studied is shown in Fig. 6. The configuration shown here differs from that described in ref. 13 in that the rectangular waveguide used for the outputs is replaced by double ridge waveguide. This change was incorporated because in order to damp transverse modes of both polarizations, four outputs rather than two would be required in an actual accelerator structure. The requirement of four outputs limits the geometrically permissable width, and the ridges are necessary to allow a cutoff frequency sufficiently low to damp the unwanted modes[14]. For the MAFIA computation reported here the damped polarisation was assured for the dangerous transverse modes by imposing a Neumann boundary condition on the $x, z$ plane at $y = 0$ and restricting the computation to the region $y > 0$.

Because the full cavity structure has three symmetry planes, it is possible to rigorously classify the modes with respect to their behavior on reflection in the symmetry planes. We shall use the designation $DD, DN$, etc. to characterize the modes. The first letter refers to reflection in the "beam" (i.e. $z$) direction and the second to reflection in the beam-waveguide plane (i.e. the $x$ direction). $D$ (for Dirichlet) means that the in plane electric field is odd under reflection and the normal electric field component even. The behavior is reversed for $N$ (for Neumann), and the behavior of the magnetic field is opposite to that of the electric field. We note that a similar symmetry characterization applies to the waveguide modes, and a cavity mode couples only to waveguide modes which share its symmetry. Modes

of a particular symmetry character can be isolated by imposing a Neumann ($N$) or Dirichlet ($D$) boundary condition on each symmetry plane and restricting the computation to the region in which all three coordinates are positive. For programs such as MAFIA, which produce many modes from a single run, this procedure is not necessarily helpful, and it was not employed for our MAFIA calculations. It was, however, employed for the SUPERFISH calculations of the ridge waveguide modes.

A total of seven MAFIA runs were carried out at seven different waveguide lengths using a mesh of more than 44000 points to represent the half of the structure with $y > 0$. Care was taken to ensure that previously fixed lattice structure not change as the waveguide length increased. Additional lattice points were simply added. Each run produces the lowest ten modes, but we shall confine our discussion here to the lowest seven. Three of the modes showed no frequency variation in the first six digits as the waveguide length was varied. We list them below.

| SYMMETRY | FREQUENCY(MHz) | CUTOFF(MHz) |
|---|---|---|
| DN | 15928.4 | 26226 |
| NN | 17274.4 | 26257 |
| DD | 24466.1 | 76231 |

The column labeled "cutoff" refers to the lowest cutoff frequency of the ridge waveguide for each symmetry type. All turn out to be $TE$ modes. Cutoff frequencies for the waveguide modes were determined by SUPERFISH computations using a 3300 point lattice filling one fourth of the ridge waveguide cross section. Symmetry conditions were imposed by boundary conditions as discussed previously. Because the frequencies of these modes are well below the cutoff of the waveguide mode to which they couple, the waveguide provides no damping for them.

The symmetry character and other properties of the modes were verified with field plots. The DN mode is the accelerator mode with 0 phase advance, the $NN$

mode the accelerator mode with $\pi$ phase advance, and the $DD$ mode is the dipole mode with 0 phase advance. The structure was designed with a 17 $GHz$ accelerator in mind so that the position of the accelerator modes is approximately correct. We note that all 0 phase advance modes have $D$ symmetry with respect to reflection in the beam direction and hence are decoupled from the principal mode of the ridge waveguide ($ND$ symmetry). The dipole modes are the principal modes that one wishes to damp, but the frequency of the mode at 0 phase advance is such that the mode is out of synchronism with a highly relativistic beam[15]. The fact that these modes are independent of the waveguide length over the range studied shows that the relevant part of the lattice structure indeed does remain fixed as the length is varied. It also shows that the exponential tails of the cutoff waveguide modes are sufficiently attenuated at the lengths studied to make their effects negligeable at the terminating conducting plane.

The remaining four modes all have $ND$ symmetry. For this symmetry the lowest waveguide cutoff frequency is 12300 $MHz$[16]. The next lowest cutoff frequency is at 65486 $MHz$. Both are $TE$ modes. Since the highest frequency that occurs among our seven modes is around 30000 $MHz$ we conclude on the basis of the observations made above that all cutoff waveguide modes can be ignored in our analysis. The MAFIA computed frequencies of the $ND$ modes for the sequence of cavity lengths are listed in Tables IV and V. The theoretical values listed along side some of the frequencies are obtained from the formulas developed in this paper. The fit points used to determine the parameters are identified in the tables by being centered between the columns of computed and theoretical values. The four modes listed correspond to just two cavity modes. Resonant frequencies and $Q$ values associated with the cavity modes and computed from four fit points as described in §2 are also listed in the tables. Fig. 7 presents a plot of the theoretical curves and the MAFIA computed points. We discuss the modes and the fits below.

The lowest frequency mode (Table IV) is a mode whose existence depends upon the slot in the accelerating iris. Its field configuration is very similar in form to that of the principal mode of the ridge waveguide. The slot appears as a continuation of the gap between the waveguide ridges, and the bulk of the cavity can be thought of as an enlargement of the inductive region of the ridge waveguide structure. These modes have come to be referred to as slot modes. They were not observed in Palmer's measurements with this model[7]. We discovered their existence and potential significance as a result of these computations. Similar modes have been observed in the structure reported in ref. 14. The resonance parameters were determined by means of the four parameter fit described in §2, using the four fit points indicated. The theoretical values were obtained by numerically solving Eq. (1.2), using the Eq.(1.3) approximation and the parameters determined by the fit points. As one might expect from the geometry of the configuration, and the nature of the mode, the $Q$ is very low (7.62) so that the mode is heavily damped as desired. We note from Table IV that the fit is essentially perfect for this mode.[17]

It was clear from observation of the field pattern that the principal excitation of the second mode listed in Table IV was in the waveguide rather than the cavity. Furthermore attempts to find a four parameter resonance fit resulted in a negative $Q$. The fit shown in the table was obtained by using the two resonance formula, Eq. (1.6). The resonance parameters $u_1$, $v_1$ were taken from the four parameter fit to the slot mode, and $u_2$, $v_2$ were taken from the fit to the mode to be discussed in the next paragraph. A linear approximation was used for $\chi(\omega)$ with parameters chosen so as to cause the solution of Eq. (1.6) to pass through the two indicated fit points. It is interesting to note that the resultant two resonance formula provides a quite respectable fit to all 28 points listed in Tables IV and V. The deviation is less than 0.15% for the first mode, less than 0.44% for the third mode (Table V),

and ranges from 0.4% to 2.6% for the fourth mode (Table V). As discussed below, the four parameter fit to the fourth mode is not particularly good either.

The third and fourth modes, listed in Table V, are two branches of the same cavity mode. It corresponds to the usual principal deflecting mode in accelerator cavities and was the mode of principal interest in this investigation. It is the $\pi$ mode counterpart of the fixed frequency $DD$ mode at 24466.1 $MHz$. The choice of waveguide lengths was intended to optimize the determination of its properties. We recall that the existence of several branches for a single cavity mode was discussed in §1 and in §3 and illustrated in Fig. 1. Accordingly, only a single set of resonance parameters is reported. The theoretical fit to the computed points is again essentially perfect on the lower branch, and parameter variation with choice of fit points on the lower branch is quite negligible.

The fact that our choice of lengths produced two branches for the same resonance enabled us to examine a number of consistency issues. First we note that the lower branch parameters produce a less than perfect set of theoretical values for the upper branch frequencies. Accordingly we computed a set of upper branch parameters based upon the last four points listed for mode 4. We found 24338.0 $MHz$ for the resonant frequency and 8.32 for $Q$. This is to be compared with 24364.2 $MHz$ and 8.70 from Table V. Using the four parameters from these fit points we determined theoretical values for the remaining three mode 4 points. While the agreement was improved, it still did not compare with the match obtained for the other three modes, and the theoretical value for the highest frequency was 128 $MHz$ high. We also computed a set of parameters from cross branch pairs of fit points, using the .918 cm and 1.118 cm waveguide lengths. Here the results were 24393.0 $MHz$ for the resonant frequency and 8.91 for $Q$. We regard these discrepancies as of methodological significance and will therefor discuss them further below. We do not consider them to be of much practical significance, however, and hence consider

them to support the overall reliability of the methodology that we are proposing. In particular we note that the cross branch method, which requires only two MAFIA runs, gives an adequate determination of cavity properties.

There is no reason in principle why one should not be able to use different waveguide lengths for cross branch determinations, for example waveguide lengths (cm) of 1.318, 1.218 from mode 4 and .918, .818 from mode 3. However, attempts to determine parameters with this point selection failed at first. The success of this kind of cross branch fit depends upon MAFIA accurately computing the guide wavelength, which in turn corresponds to an accurate determination of the waveguide cutoff frequency. This issue having been raised, we investigated the sensitivity of our parameters to the value specified for the cutoff. We were pleased to find that for a mode 3 determination, a 1% decrease in the cutoff caused only a .048% increase in $Q$ and a .0034% decrease in resonant frequency. (As noted in footnote 16 we consider our cutoff determination to be within 1% of the correct value.) One can in fact determine a MAFIA computed value of the guide wavelength from the computed points and the four parameter fit to the lower branch. We explain the procedure by means of an example. First note that at a waveguide length of 1.318 cm the mode 4 frequency is 24582.7 $MHz$. The four parameter fit of the lower branch can be used to determine a waveguide length which produces the identical frequency for mode 3. The two lengths should then differ by one half a guide wavelength. One can then check to see if the cutoff determined by this procedure agrees with the one used in the four parameter fit. Adjusting until this is the case we find that the required length for mode 3 is .69196 cm, and the self consistent cutoff is 11620.8 $MHz$. With this modified value of the cutoff and using the same set of fit points as used previously (including the set mentioned in the opening sentence of this paragraph), we obtain the following values:

| | FREQUENCY(MHz) | Q |
|---|---|---|
| Lower Branch (Mode 3) | 24357.8 | 8.72 |
| Upper Branch (Mode 4) | 24352.9 | 8.47 |
| Cross Branch (Two lengths) | 24373.1 | 8.54 |
| Cross Branch (Four lengths) | 24352.4 | 8.51 |

We see that the four length cross branch fit now produces consistent results, and that the change in the lower branch determined parameters due to the cutoff change is minimal. The overall mode 3 fit with mode 3 determined parameters is somewhat degraded as compared to Table V. Because we believe 12300 $MHz$ to be a more accurate value for the cutoff, we used it for the computations Table V.[18] The mode 4 overall fit is improved using mode 3 parameters and even more so using mode 4 parameters. The highest frequency mode at the $D$ equals .668 cm., however, is still 93 $MHz$ high in the best case.

Because it has some bearing on the comparatively large discrepancy for the highest mode 4 frequencies, we briefly comment on the remaining three highest frequency modes produced in the MAFIA runs. Recalling that we have so far confined our attention to the lowest seven modes, we refer to them as modes 8, 9, and 10 in order of increasing frequency. There is a marked degradation in the MAFIA accuracy parameters[19] for these modes and also to a lesser extent for the highest frequency modes listed in Table V, so that parameters determined are quite tentative. The 8'th mode is $DN$ with resonant frequency 28400 $MHz$ and $Q$ 3.8. The 10'th mode is $NN$ with resonant frequency 31900 and $Q$ 76. Note that modes of these symmetries now exhibit external loading because the resonant frequencies are now above the waveguide cutoff of corresponding symmetry. The 9'th mode is a clear $ND$ doublet. We have not attempted a two resonance analysis both because of the low accuracy and because of a somewhat inadequate number of points. However the resonant frequencies appear to be at 30800 $MHz$ and 31900 $MHz$. $ND$ resonances

at these frequencies would be expected to depress the highest frequency modes in Table V and their presence is almost certainly the primary reason for the observed remaining discrepancies.

We concluded from the above analysis that the configuration studied above satisfactorily damps the lowest two deflecting modes. The $Q$ of the accelerating mode remains high despite the fact that its resonant frequency is well above the cutoff of the principal waveguide mode. The decoupling of the accelerating mode depends upon the symmetry mismatch between it and the principal waveguide mode. In a fabricated cavity some departure from symmetry is inevitable, leading to leakage of the accelerating mode through the waveguide. We estimate that the coupling of the accelerating mode should be reduced from that of the deflecting mode by roughly the square of the departure from symmetry. Thus a readily achievable 2 % limit on departure from symmetry should lead to a $Q$ in excess of 20000. One could of course raise the cutoff frequency to a value above the accelerating mode frequency. This is most easily accomplished by increasing the gap between the ridges in the wave guide. Such a procedure increases the $Q$ of the dipole mode to 13.9 (as determined by an analysis of the sort carried out in this section), a value which is still considered to be satisfactorily low. A more serious concern is that it leaves the slot mode undamped. It is possible, however, that the transverse impedance of this mode is sufficiently low that it may not need to be damped. We are currently applying our method to other designs of damped accelerator cavities including circumferential slot designs[7] as they may have have fabricational advantages.

## 5. CONCLUDING REMARKS

As indicated in the preceding section, the methods developed in this paper are currently being applied to a variety of design problems. Much of this is being carried out without direct confrontation with experiment. We have been relying principally upon internal consistency as evidence for the reliability of the results. It should be

mentioned that not all of our applications have presented as consistent a picture as that reported here, but the results have always been useful and informative. The limited confrontation with experiment has been encouraging, but has not been carried out far enough to be definitive. It should also be noted that, for very low $Q$, standard methods of measurement may be unreliable. For example, the lower the $Q$ the more difficult it is to detune the cavity sufficiently to implement the detuned short method[10].

We believe that the waveguide model adequately demonstrates the theoretical reliability of the method when the approach of the resonant frequency to the wave guide cutoff is not excessively close and when the resonances are well enough separated. For the waveguide model the ratio of the lowest resonant frequency (coupled) to the cutoff is 1.228, and the ratio of the frequency of the resonance studied to the next higher resonance is about .63. Modifications of the model to broaden the range studied are planned for the future. Situations requiring a two resonance analysis are likely to become important in the study of higher modes, and an extended waveguide model should be helpful in developing it.

For situations which we consider to be theoretically validated by the wave guide model, problems with computer implementation may still arise. We do not yet have a systematic understanding of the level of computer accuracy required to obtain consistent results. The work reported in §4 shows that the required level is achievable, but unanticipated problems have arisen in other situations. Computer modeling of cavity geometry is generally not exact. For example curved surfaces are typically replaced by polyhedra. While this has not been a significant problem for the study of mode spectra and structure, imprecise modeling of the output structure can have a significant effect upon $Q$. This is because external coupling is quite sensitive to the details of the output design.

Methods following the general approach described in this paper are still under development. Our aim is to develop and validate it to the point that it can be routinely and reliably applied with a minimum expenditure of computer and analysis time. As we have shown in this paper, our method is a useful tool even in its present stage.

## ACKNOWLEDGEMENTS

It is a pleasure to thank Z. D. Farkas, R. Foukes, R. Palmer and P. Wilson helpful discussion, and X. T. Lin for assistance in the preparation of the graphs. We also wish to thank the Stanford Linear Accelerator Center, where a portion of this research was carried out, for hospitality and support.

## FOOTNOTES

1. T. Weiland et al. DESY Report M-86-07, June 1986.
2. T. Weiland, Nuclear Instruments and Methods **216**, 329 (1983).
3. K. Halbach and R. F. Holsinger, Particle Accelerators **7**, 213 (1976).
4. J. C. Slater, Microwave Electronics (Van Nostrand, New York, 1950) (Bell Telephone Laboratory Series) Ch. 5 §1.
5. R. L. Gluckstern and R. Li, Proceedings of the 1988 LINAC Conference, CEBAF report 89-001, (1989) pp. 356-358. Also T. Kageyama, KEK-Report 89-4 (1989). Both of these papers determine the location of the detuned short by an extrapolation procedure, which yields a frequency independent position. For low values of $Q_{ext}$, the frequency dependence of its location over the resonance width can have a substantial effect. (see reference 10)
6. Y. Goren and David Y. L. Yu, SLAC/AP-73 (1989).
7. R. B. Palmer, Proceedings of the Summer study on High Energy Physics in the 1990's, Snowmass, Colo., Edt. S. Jenson (World Scientific, Singapore, 1989), pp. 638-641.
8. The choice of the output origin as a reference plane is really arbitrary but desireable for most effective application of the method to be described. One of the features of our method is its avoidance of the concept of "detuned short" as a means of determining the reference plane.
9. The resonant frequency defined by Slater's method is related to ours by

$$\omega^2 = u^2(1 + 1/4Q^2)$$

His $Q$ is $\omega/2v$ rather than $u/2v$. The relation is identical to that which pertains to an L. C. R. series resonant circuit when one compares the conventional

definitions with those which one would obtain from the damped oscillation solution.

10. We plan to discuss the relation between the two methods and compare their accuracy in a future publication.
11. N. Marcuvitz. Waveguide Handbook, MIT Radiation Laboratory Series V-10, (McGraw Hill, 1951, Reprinted with revisions in IEE Electromagnetic Waves Series V-21 1986).
12. Microwave Transmission Data, T. Moreno, (Sperry Gyroscope Company, Inc., Great Neck, NY, 1944) p. 102.
13. Reference 7, especially 3.1 and Fig. 4.
14. H. Deruyter, H. Hoag, A V. Lisin, G. A. Loew, R. B. Palmer, J. M. Paterson, C. E. Rago, J. W. Wang; Damped Accelerator Structures for Future Linear $e^{+-}$ Colliders, SLAC-PUB-4865 (Mar. 1989). To be published in the Proceedings of the IEEE 1989 Particle Accelerator Conference.
15. See reference 7 §2 and Fig. 2. The mode designated (c) in Fig. 2 corresponds to the dipole 0 mode.
16. The principle mode cutoff was determined using SUPERFISH, with the 3300 point mesh mentioned in the text. (The actual value was 12301 $MH_z$). Comparison with coarser meshes showed that the cutoff frequency decreased with decreasing mesh size. Using the values to produce a crude extropolation to zero mesh size yields 12184 $MH_z$ for the cutoff frequency. We also computed the cutoff using the analytic approximations in reference 11. A computation based upon formulas in §8.1 yielded 12286 $MH_z$, while one based on those in §8.8 yielded 12292 $MH_z$. We believe the figure 12300 $MH_z$ used in the text to be high, but by no more than 1%.
17. It should be noted, however, that the parameters are very sensitive to the frequencies of the points, especially when a set of adjacent points is used for

fitting. Due to the fact that the resonant frequency is very close to the waveguide cutoff, the entire range of phase covered is only .42 rad which is much less than the optimum range of 1.5 to 2 rad. The associated frequency differences are small and even round off has a noticeable effect. The range of lengths chosen for the study were determined with the dipole mode in mind (Table V), as the existence of the slot mode had not been anticipated.

18. In connection with a different problem, we used MAFIA to compute resonant frequencies of a ridge waveguide cavity. Resonant frequencies were found for one, two, and three half wavelengths of the fundamental TE(ND) waveguide mode. Using a mesh size comparable to that used for the cavity calculations reported in this paper, we found that the computed cutoff frequency decreased as the cavity resonant frequency increased, with an overall variation of 5.7% observed. All cutoff frequencies increased and the overall variation decreased to 0.16% when the number of mesh points was increased by a factor of 28. The extropolated cutoff agreed quite well with SUPERFISH, URMEL, and Marcuvitz based results. These observations make more understandable the fact that our results appear to be more consistent if we allow the cutoff frequency to decrease for the analysis of the higher frequency modes.

19. Our MAFIA runs were restricted to the lowest ten modes. The decrease in the accuracy parameters is characteristic of MAFIA for the upper modes of a run and could be avoided for modes 8, 9, and 10 by including an additional number of modes in the run.

## FIGURE CAPTIONS

Figure 1. Typical examples of relative frequency f plotted as a function of relative length r. The frequency f is normalized to the frequency of the uncoupled cavity mode, and the waveguide length is normalized to one half the cutoff wavelength. The cavity mode is sufficiently isolated, so that other cavity modes do not have a significant effect over the frequency range shown. Figure 1a represents a weakly coupled case. The dashed curves are the uncoupled waveguide resonances. Figure 1b shows the evolution of the plot as the coupling is increased to a moderate value.

Figure 2. Behavior of the phase variable $\psi$ as a function of relative frequency f. The particular example shown corresponds to the lowest frequency curve of Figure 1b, with the proviso that the negative $\psi$ portion, which occurs for f > 1.0, is to be ignored. The $\psi - \omega$ curves corresponding to the successive higher frequency curves of Figure 1b are obtained by adding $\pi$, $2\pi$, etc. to the ordinates of the above curve, and for these higher curves the entire frequency range shown is relevant. The droop in the curve that becomes evident as f approaches 1.4 is indicative of the presence of another cavity mode at somewhat higher f.

Figure 3. A typical example of the dependence of $-\frac{1}{2}d\psi/df$ on the relative frequency. Again the example is that used for Figure 1b and Figure 2. The peak of this curve occurs at the resonant f and $-\frac{1}{2}f\frac{d\psi}{df}$ is approximately equal to $Q_{ext}$.

Figure 4. The waveguide model

Figure 5. (a) Equivalent circuit for the waveguide model with outgoing wave boundary condition. The distance of the terminating characteristic impedance from the shunt susceptance is arbitrary. (b) Equivalent circuit for the waveguide model with terminating short at distance $D$ from the output window.

Figure 6. Schematic drawing of the cavity and waveguide structure used for the calculations of §4.

Figure 7. Frequencies f of the lowest four (ND symmetry) coupled cavity-waveguide modes of the model discussed in §4 plotted as a function of waveguide length D. The plotted points are obtained from the seven MAFIA runs. The points designated by $\times$ are the fit points (i.e. the points used to determine the parameters), other points being designated by $+$. The curves are obtained from the theory described in the text and used to compute the points in the (Th) columns of Table IV and Table V.

TABLE I: Waveguide cavity results.

This table compares results obtained from solving the complex frequency eigenvalue problem (labled exact) with those obtained from the three parameter (3 p) and four parameter (4 p) formulas. The right hand column lists the frequencies chosen for these formulas, the first three being used in the three parameter formula.

| d/a | u (exact) | u (3p) | u (4 p) | Q (exact) | Q (3 p) | Q (4 p) | Fr's |
|---|---|---|---|---|---|---|---|
| .3 | .98071 | .98071 | .98071 | 216.35 | 216.56 | 216.35 | .978 |
| | | | | | | | .980 |
| | | | | | | | .982 |
| | | | | | | | .984 |
| .4 | .96417 | .96406 | .96417 | 62.69 | 63.17 | 62.69 | .95 |
| | | | | | | | .96 |
| | | | | | | | .97 |
| | | | | | | | .98 |
| .5 | .94240 | .94175 | .94240 | 23.99 | 24.03 | 23.99 | .92 |
| | | | | | | | .93 |
| | | | | | | | .94 |
| | | | | | | | .95 |
| .6 | .91639 | .91614 | .91637 | 11.145 | 11.92 | 11.14 | .90 |
| | | | | | | | .915 |
| | | | | | | | .93 |
| | | | | | | | .945 |
| .65 | .90192 | .89866 | .90180 | 8.01 | 8.83 | 7.99 | .87 |
| | | | | | | | .89 |
| | | | | | | | .91 |
| | | | | | | | .93 |
| .7 | .88618 | .8755 | .8857 | 5.89 | 6.62 | 5.82 | .84 |
| | | | | | | | .86 |
| | | | | | | | .88 |
| | | | | | | | .90 |
| .75 | .8684 | .8573 | .8661 | 4.40 | 5.52 | 4.28 | .83 |
| | | | | | | | .85 |
| | | | | | | | .87 |
| | | | | | | | .89 |

Table II: Waveguide Cavity Results Based Upon Two Waveguide Lengths.

Like Table I, this table compares exact frequencies and Q's with those obtained from the four parameter formula. Here the four data points required are obtained from runs at two waveguide lengths using pairs of data points from adjacent branches, the same branch pairs being used for each length. In Table 1, the four data points are from a single branch but from runs at four cavity lengths.

| d/a | u (exact) | u (4 p) | Q (exact) | Q (4 p) | (d/a) values | Branches |
|---|---|---|---|---|---|---|
| .30 | .98071 | .98071 | 216.35 | 216.35 | 1.08 | 1, 2 |
| | | | | | .95 | |
| .40 | .96417 | .96417 | 62.69 | 62.68 | 1.05 | 1, 2 |
| | | | | .95 | | |
| .50 | .94240 | .94238 | 23.99 | 23.96 | 1.12 | 1, 2 |
| | | | | | 1.02 | |
| .60 | .91639 | .91615 | 11.45 | 11.01 | 1.31 | 1, 2 |
| | | | | | 1.26 | |
| .60 | | .91633 | | 11.13 | 2.30 | 2, 3 |
| | | | | | 2.20 | |
| .65 | .90192 | .90314 | 8.01 | 7.69 | 1.63 | 1, 2 |
| | | | | | 1.58 | |
| .65 | | .90163 | | 7.98 | 2.50 | 2, 3 |
| | | | | | 2.30 | |
| .70 | .88618 | .88516 | 5.89 | 5.90 | 2.40 | 2, 3 |
| | | | | | 2.60 | |
| .75 | .8684 | .8650 | 4.40 | 4.33 | 2.50 | 2, 3 |
| | | | | | 2.70 | |

Table III: Quality of Fit

This table shows the range in linewidth over which the four parameter representation is within 0.01 rad of the correct phase for the wave guide model. The figures in parentheses refer to the range for a 0.1 discrepancy.

| d/a | Range of fit (line widths) |
|---|---|
| 0.3 | >84 |
| 0.4 | >23 |
| 0.5 | 7.5 |
| 0.6 | 3.2 |
| 0.65 | 2.4 (>4) |
| 0.7 | 1.2 (>2.8) |
| 0.75 | 0.86 (>2.1) |

Table IV

Computed frequencies of the first and second mode for a series of waveguide lengths compared to a theoretical representation. Single entries correspond to fit points used to determine the parameters for the theoretical representation. Only the first mode is a cavity mode. The resonant frequency and Q were determined by means of the four parameter representation, using the indicated fit points as discussed in § 2.

| Mode 1 Frequencies ($MH_z$) (Comp) | (Th) | Wave Guide Length (cm) | Mode 2 Frequencies ($MH_z$) (Comp) | (Th) |
|---|---|---|---|---|
| 13382.9 | | .668 | 18826.0 | 18832.0 |
| 13270.4 | 13270.4 | .818 | 17781.6 | 17782.7 |
| 13237.1 | | .868 | 17484.6 | |
| 13205.5 | 13205.5 | .918 | 17210.2 | 17209.5 |
| 13093.3 | | 1.118 | 16303.6 | |
| 13044.1 | 13044.0 | 1.218 | 15943.5 | 15845.8 |
| 12998.5 | | 1.318 | 15632.0 | 15637.8 |
| Resonant Frequency ($MH_z$) | 13026.3 | | | |
| Q | 7.62 | | | |

Table V

Computed frequencies of the third and fourth modes for a series of waveguide lengths compared to the four parameter representation. Single entries correspond to fit points used to determine the four parameters. These two resonances correspond to two branches of the same cavity mode. The resonant frequency and Q emerge from the four parameter fit. Possible reasons for the relatively poor agreement in the mode 4 case are discussed in the text.

| Mode 3 Frequencies ($MH_)$ | | Wave Guide Length (cm) | Mode 4 Frequencies (MH) | |
|---|---|---|---|---|
| (Comp) | (Th) | | (Comp) | (Th) |
| 24388.6 | | .668 | 30043.5 | 30486.3 |
| 23734.7 | | .818 | 28013.2 | 28202.6 |
| 23500.8 | | .868 | 27458.0 | 27598.6 |
| 23252.1 | | .918 | 26960.9 | 27066.8 |
| 22102.9 | 22103.0 | 1.118 | 25498.0 | 25543.3 |
| 21476.1 | 21476.4 | 1.218 | 24999.8 | 25038.7 |
| 20856.5 | 20857.4 | 1.318 | 24582.0 | 24622.6 |
| Resonant Frequency ($MH_z$) | 24364.2 | | | |
| Q | 8.70 | | | |

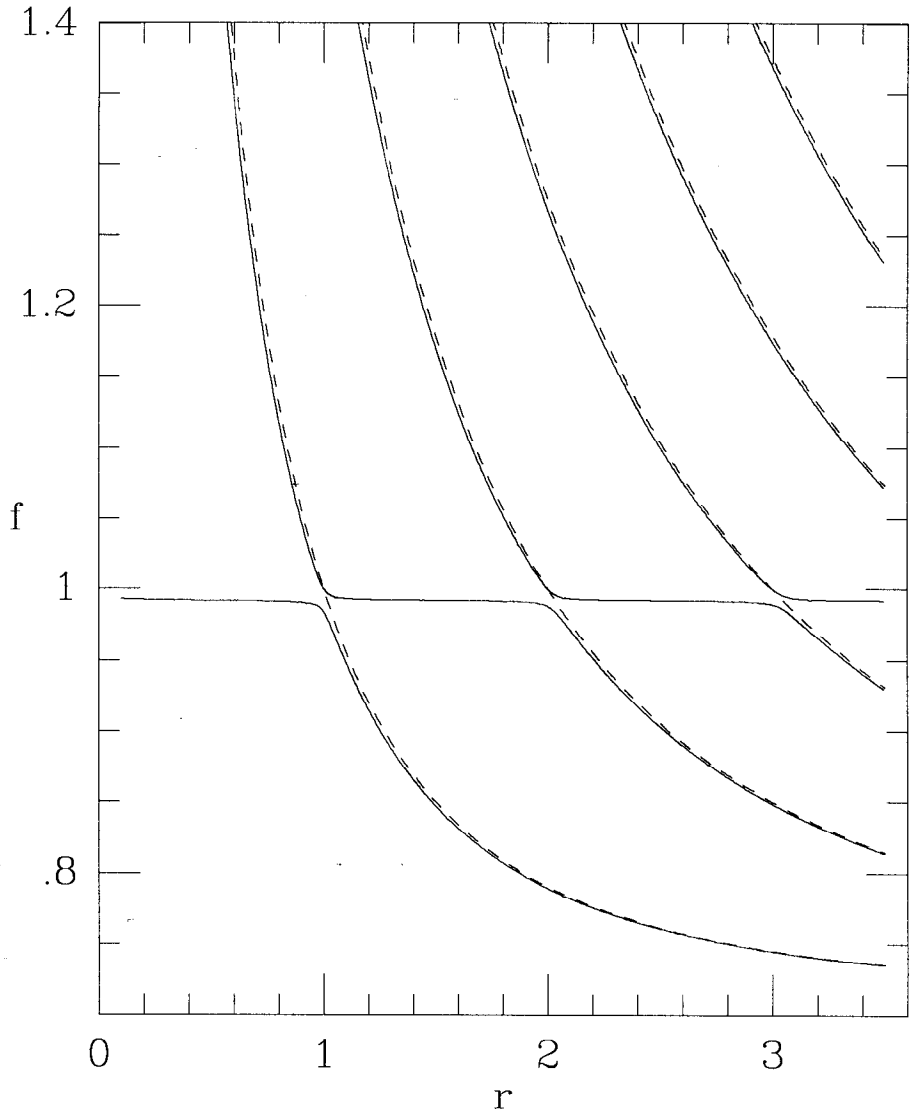


Fig. 1a

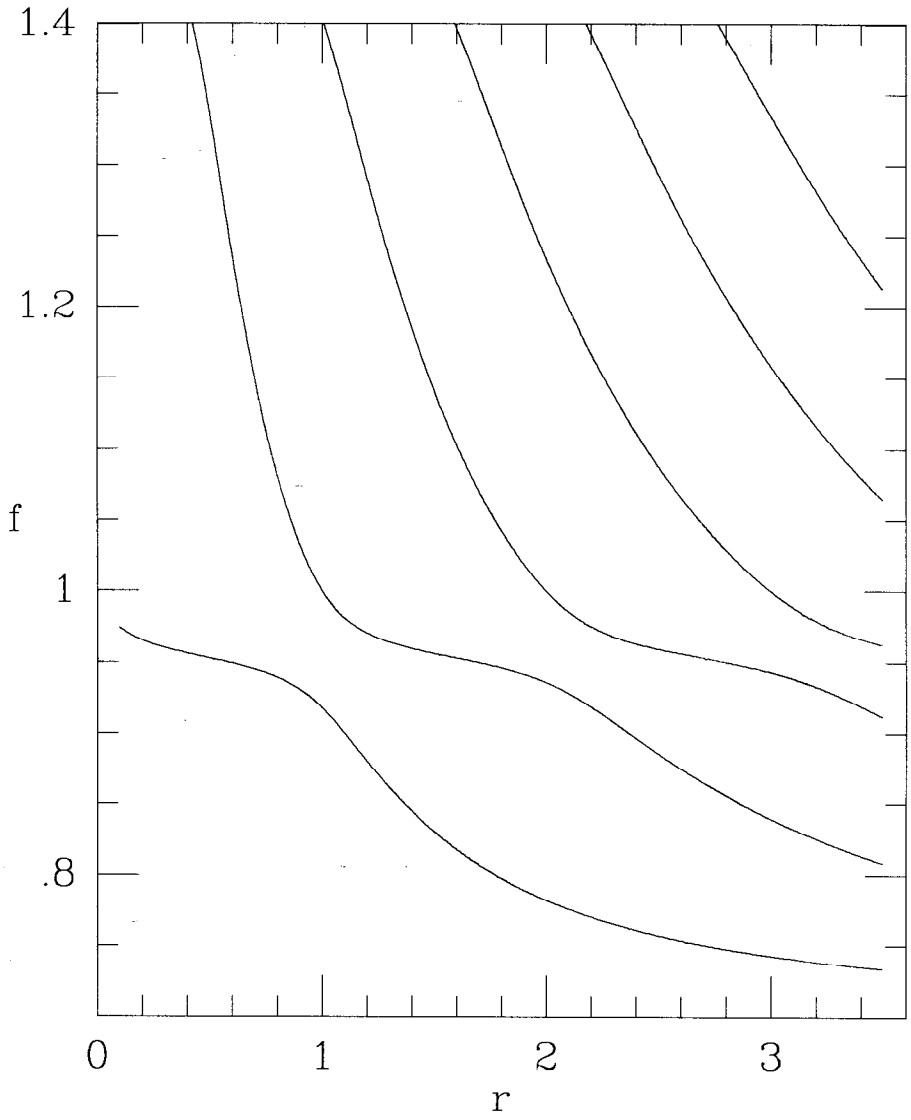


Fig. 1b

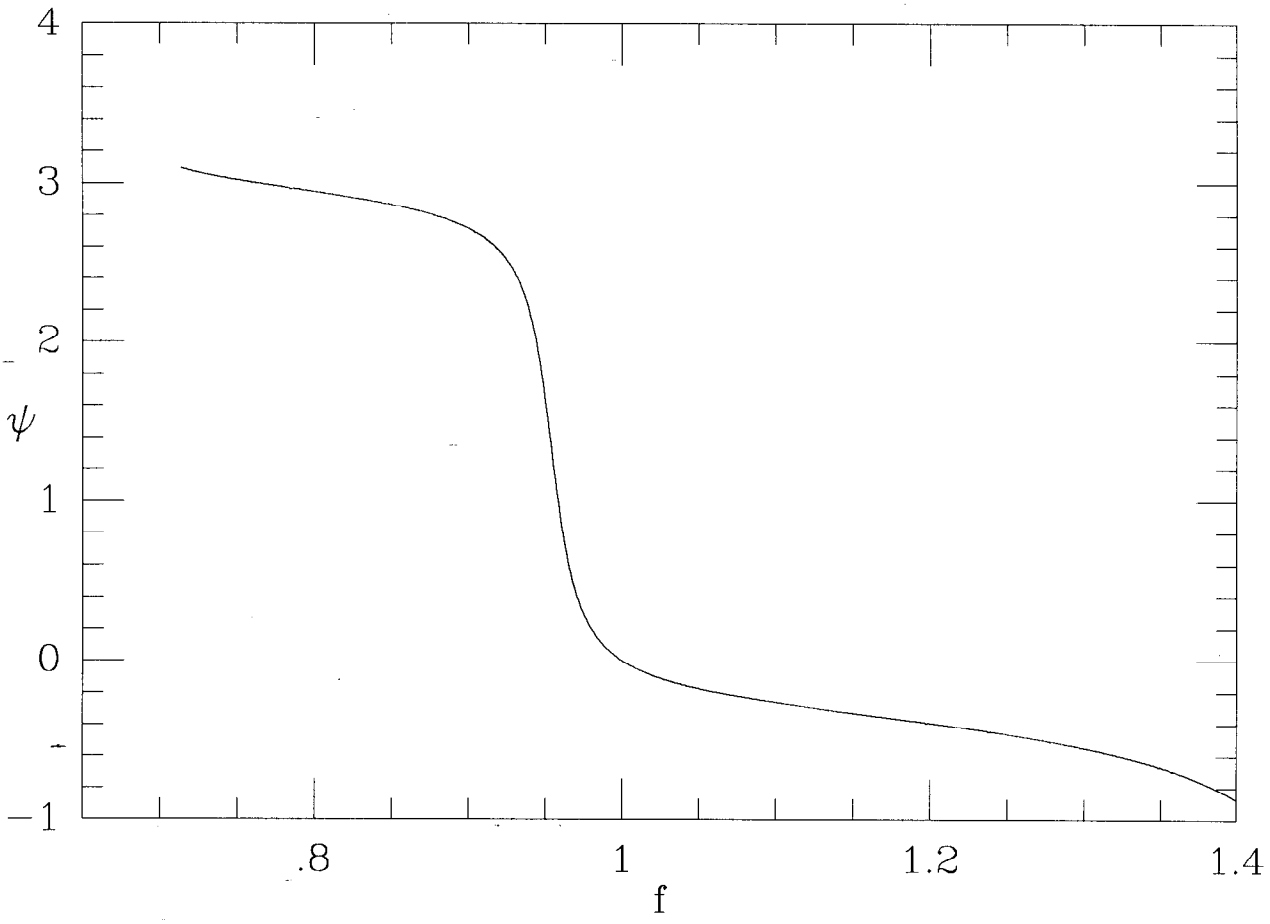


Fig. 2

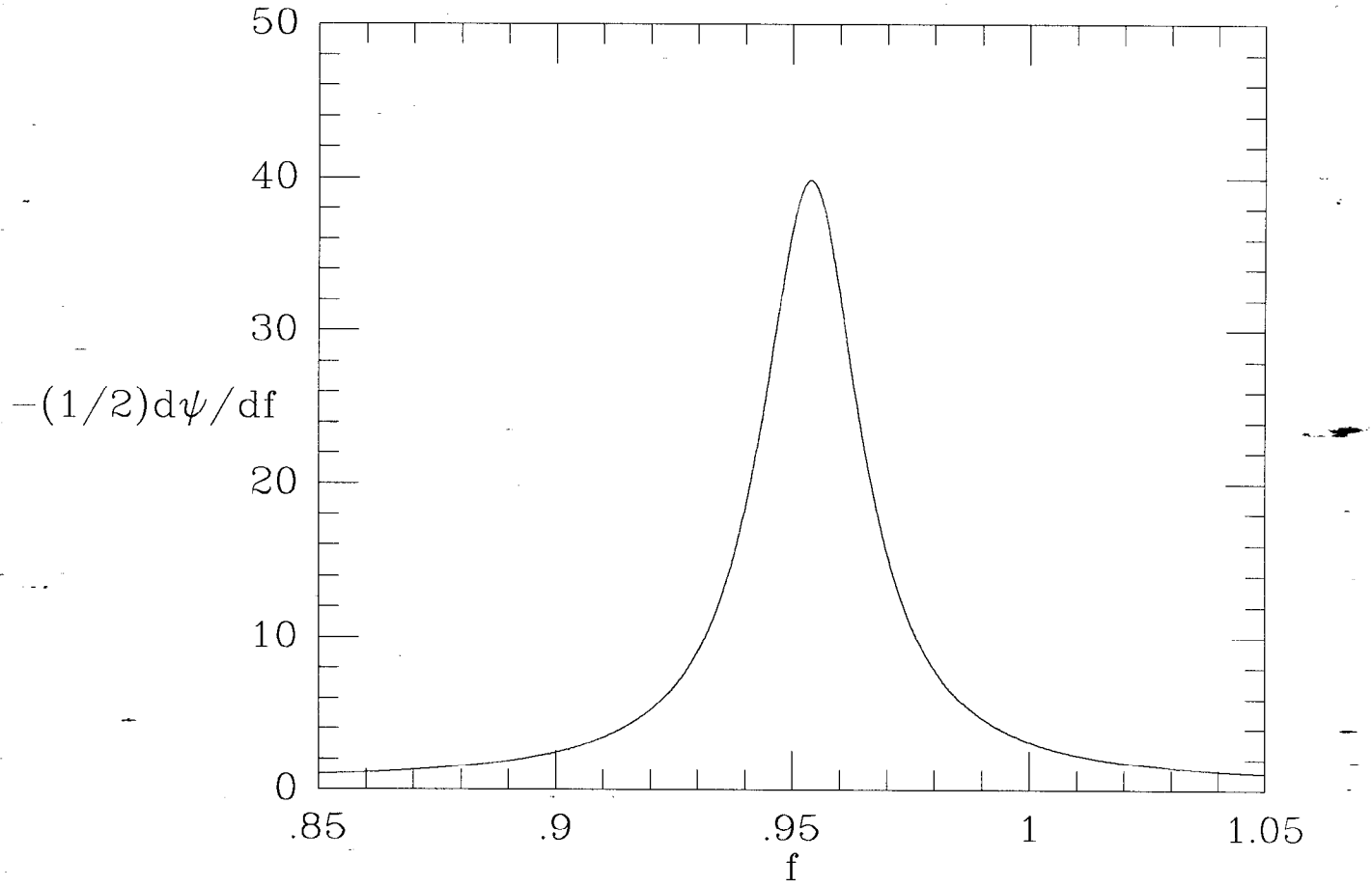


Fig. 3

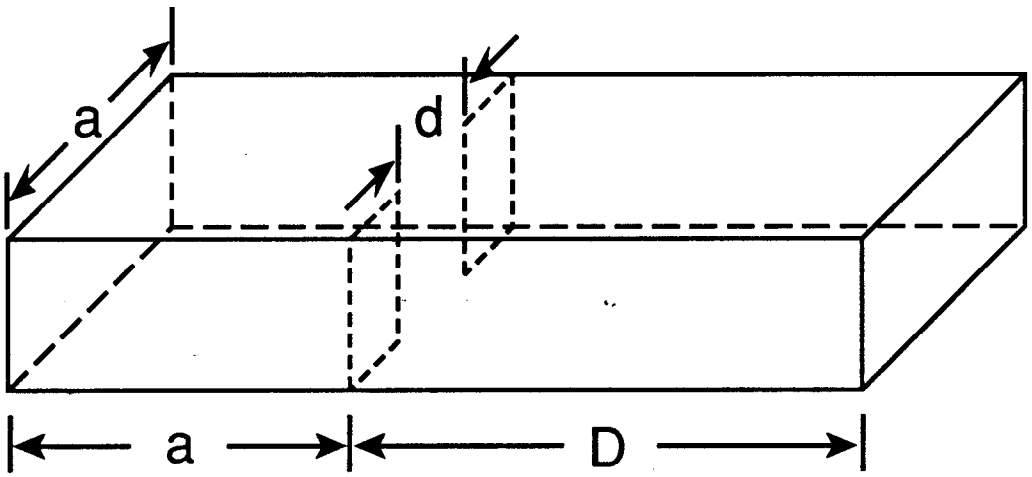


Fig. 4

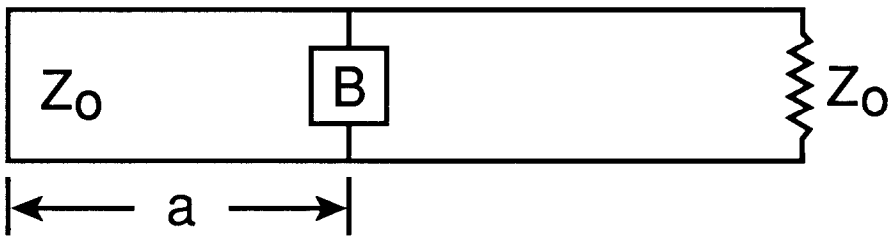


(a)

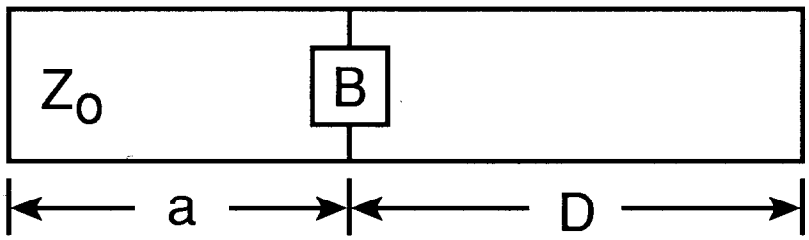


(b)

Fig. 5

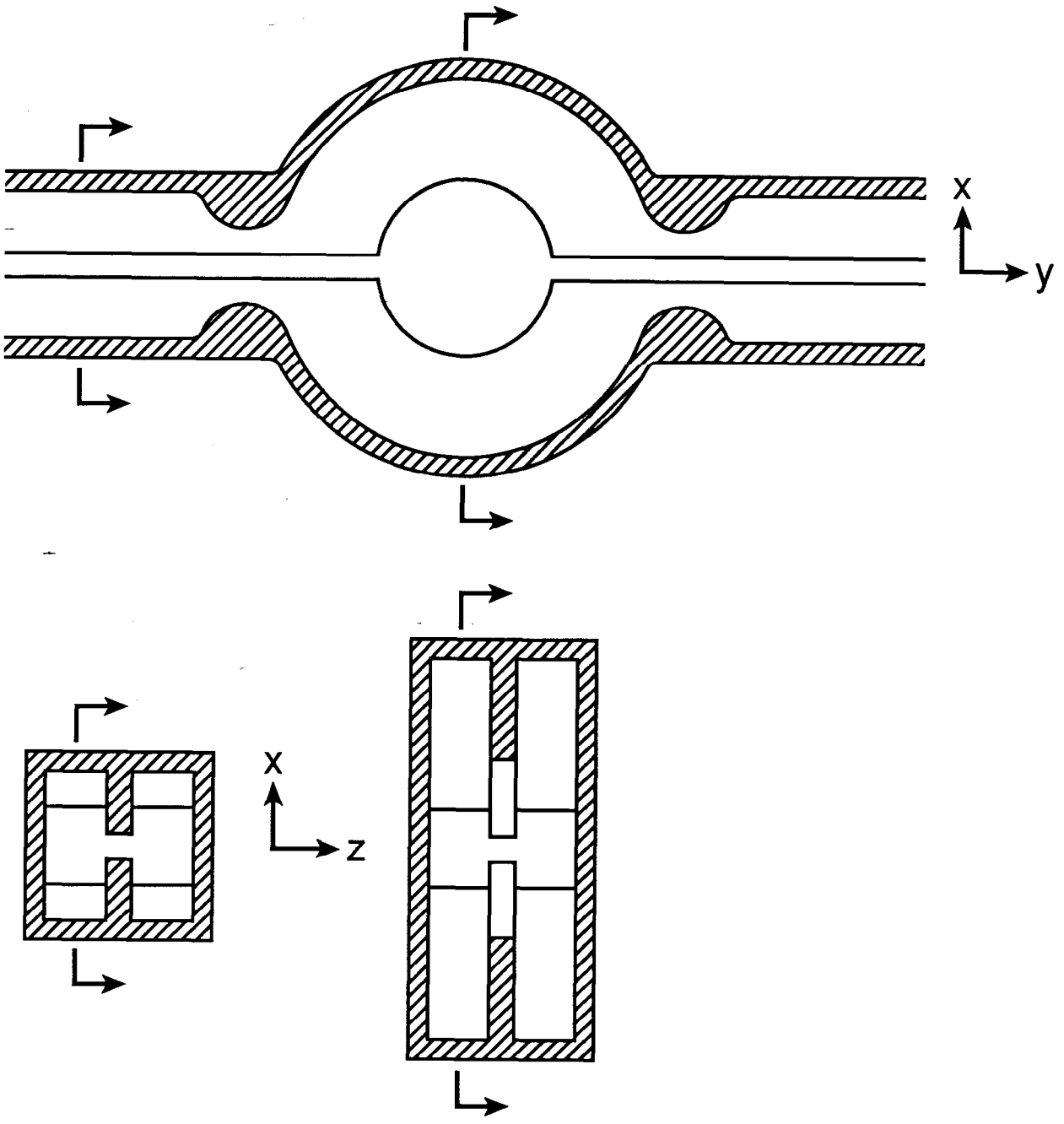


Fig. 6

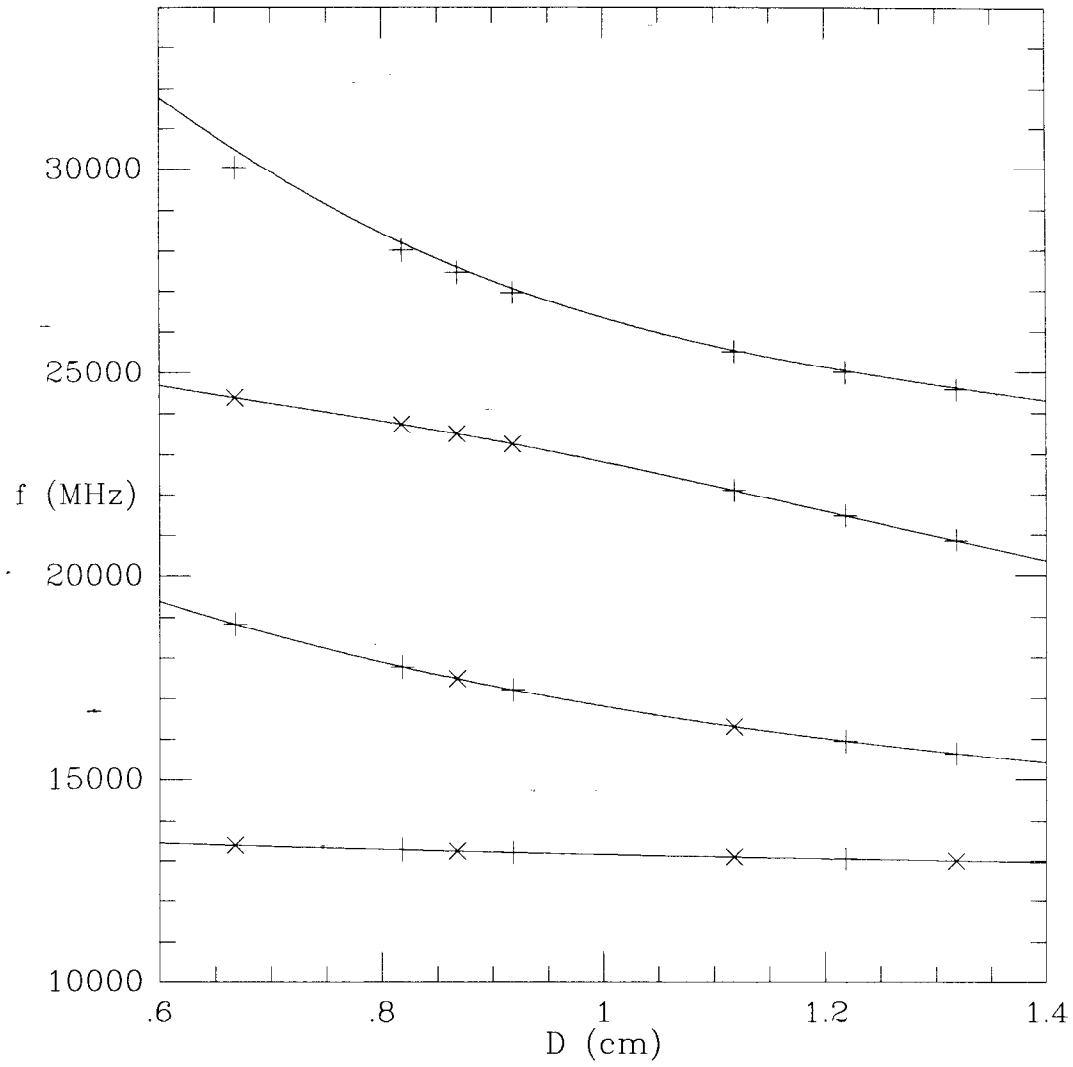


Fig. 7